Exploratory Research and Hypothesis in Medicine **2025** vol. 10(1) | 36–48
DOI: 10.14218/ERHM.2024.00033

Original Article

E64FC26, a Protein Disulfide Isomerase Inhibitor, Ameliorates Articular Cartilage Damage and Disease Severity in a Mouse Model of Rheumatoid Arthritis

Haiyan Zhao[1], Ting Wang[1], Luna Ge[1], Yuang Zhang[1], Ruojia Zhang[1], Guanhua Song[2], Jihong Pan[1], Lin Wang[1*] and Jinxiang Han[1*]

[1]*Biomedical Sciences College & Shandong Medicinal Biotechnology Centre, Key Lab for Biotech-Drugs of National Health Commission, Key Lab for Rare & Uncommon Diseases of Shandong Province, Shandong First Medical University & Shandong Academy of Medical Sciences, Jinan, Shandong, China;* [2]*Institute of Basic Medicine, Shandong First Medical University & Shandong Academy of Medical Sciences, Jinan, Shandong, China*

Received: September 24, 2024 | **Revised:** November 21, 2024 | **Accepted:** December 04, 2024 | **Published online:** January 25, 2025

Abstract

Background and objectives: Protein disulfide isomerases (PDIs) are essential enzymes that facilitate the proper folding of proteins and maintain protein quality within the endoplasmic reticulum. Dysregulation of PDIs has been correlated with numerous disorders, including cancer and rheumatoid arthritis (RA). E64FC26 (EFC), a small molecule that inhibits a wide range of PDI family members, has shown promise as a therapeutic agent in oncology. However, its effects on RA have not yet been studied. This research investigates the efficacy of EFC as a potential treatment for RA.

Methods: To investigate EFC's effects on RA fibroblast-like synoviocytes, several assays were employed, including Cell Counting Kit-8 for cell viability, EdU for cell proliferation, Transwell for migration and invasion, TUNEL for apoptosis, and *in vitro* tube formation assays for angiogenesis. Flow cytometry was used to assess apoptosis in detail. Cytokine production was analyzed using ELISA and real-time polymerase chain reaction. *In vivo*, a collagen-induced arthritis model was developed in DBA mice to evaluate EFC's effects on inflammation, disease progression, and bone damage. RNA sequencing was utilized to identify the molecular pathways influenced by EFC treatment.

Results: EFC exhibited significant anti-inflammatory effects on RA fibroblast-like synoviocytes, reducing cell proliferation, migration, invasion, angiogenic activity, and cytokine secretion, while simultaneously promoting apoptosis. *In vivo* experiments using the collagen-induced arthritis mouse model showed that EFC alleviated inflammation, slowed disease progression, and preserved joint and bone integrity. RNA sequencing data suggested that EFC acts through pathways associated with inflammation and apoptosis regulation.

Conclusions: The findings of this research underscore EFC's therapeutic potential in managing RA. These results pave the way for the development of inhibitors targeting the PDI family as innovative treatments for RA.

Keywords: Unfolded protein response; E64FC26; Apoptosis; Inflammation; Protein disulfide isomerases inhibitor; Rheumatoid arthritis.

***Correspondence to:** Jinxiang Han and Lin Wang, Biomedical Sciences College & Shandong Medicinal Biotechnology Centre, Key Lab for Biotech-Drugs of National Health Commission, Key Lab for Rare & Uncommon Diseases of Shandong Province, Shandong First Medical University & Shandong Academy of Medical Sciences, Jinan 250117, Shandong, China. ORCID: https://orcid.org/0000-0003-0227-9757 (JH); https://orcid.org/0000-0002-5478-0212 (LW). Tel: +86-531-59567360 (JH); +86-0531-59567360 (LW), Fax: +86-531-59567355 (JH); +86-0531-59556660 (LW), E-mail: samshjx88@sina.com (JH); linwang@sdfmu.edu.cn (LW)

How to cite this article: Zhao H, Wang T, Ge L, Zhang Y, Zhang R, Song G, *et al.* E64FC26, a Protein Disulfide Isomerase Inhibitor, Ameliorates Articular Cartilage Damage and Disease Severity in a Mouse Model of Rheumatoid Arthritis. *Explor Res Hypothesis Med* 2025;10(1):36–48. doi: 10.14218/ERHM.2024.00033.

Introduction

Rheumatoid arthritis (RA) is an inflammatory disease that causes progressive joint destruction, including synovial inflammation and cartilage degradation.[1] During disease progression, fibroblast-like synoviocytes (FLSs) become activated, producing excessive cytokines that contribute to pannus formation and subsequent bone erosion.[2] Current RA therapies primarily aimed to control inflammation and achieve clinical remission.[3] However, approximately 30–40% of patients fail to respond adequately to available treatments.[4] This emphasizes the critical importance of developing novel RA therapy techniques.

Protein disulfide isomerases (PDIs) are a class of related oxidoreductases that assist in protein folding in the endoplasmic reticulum (ER). These enzymes catalyze the synthesis, rearrangement, and elimination of disulfide bonds, collaborating with molecular chaperones to fold secretory proteins and control misfolded ones via refolding or destruction. Notably, PDIs are integral to the proteostasis network, a system that links protein folding to cellular homeostasis mechanisms in response to environmental or metabolic demands. As such, PDIs play an important role in maintaining ER protein balance and supporting multiple physiological activities, including glucose metabolism, calcium storage, organelle biogenesis, and adipogenesis.[5] Dysregulation of PDI activity has been implicated in various pathological conditions,[6] suggesting that PDI inhibition may hold therapeutic potential for disease management.

E64FC26 (EFC) is a potent pan-inhibitor of PDIs, targeting several members of the PDIA family, including PDIA1, PDIA3, PDIA4, TXNDC5, and PDIA6. It acts as a covalent small-molecule inhibitor by binding irreversibly to active cysteine residues in the catalytic domain of PDIs as o-quinones.[7] This binding prevents PDIs from returning to their oxidized monomeric state, disrupting the formation of disulfide bonds in unfolded proteins and impeding misfolded protein remodeling. Consequently, this inhibition leads to an increase in improperly folded proteins. EFC has demonstrated therapeutic efficacy in diseases such as multiple myeloma,[8,9] and research suggests that PDIs, including TXNDC5 and PDIA3,[10–13] are also implicated in RA pathology.

Studies have highlighted PDIs' involvement in modulating immune cell functions and inflammatory responses in RA. Research by Wang *et al*.[14] demonstrated that PDI overexpression promotes the production of cytokines that drive inflammation and synovial proliferation of cells, highlighting its role in disease development. Furthermore, clinical investigations have shown that PDI expression levels are significantly elevated in the synovial tissues of RA patients compared to healthy controls, suggesting a pathogenic role for these enzymes. Inhibition of PDI activity has emerged as a promising therapeutic approach. Yang *et al*.[15] provided evidence for PDI's potential as a therapeutic target by showing that inhibiting PDI can successfully lower inflammation and joint degeneration in RA model mice. Given these findings, it is reasonable to hypothesize that EFC may also exhibit therapeutic benefits in RA.

The goal of this study was to examine EFC's anti-inflammatory qualities in RA and investigate its potential for clinical use.

Materials and methods

Cell culture and cell treatment

Synovial tissue samples were obtained from 12 individuals undergoing joint replacement surgery (six females, six males; age range: 48–66 years; mean age: 57 years). All participants satisfied the rheumatoid arthritis classification criteria established by the American College of Rheumatology in 1987.[16] All patients provided written informed consent in accordance with the Declaration of Helsinki, and the Shandong Medical and Biotechnology Center's Institutional Review Board authorized the study (approval number: SMBC2020-03). Synovial tissues were sectioned and digested with collagenase III and II (Solarbio, Hangzhou, China) for 6 h (Gibco, Carlsbad, CA, USA).

Initial cytotoxicity assays were conducted to determine the optimal concentration of E64FC26 (EFC). RA FLSs were seeded in 24-well plates at a density of 3–5 × 10^5 cells per well and subjected to a 12-h serum starvation phase. Treatment groups were then exposed to varying concentrations of EFC for 6 h,[17,18] after which cells were stimulated with interleukin-1β (IL-1β, 10 ng/mL; Solarbio, Beijing, China) for 20 h.

Peripheral blood mononuclear cells (PBMCs) were isolated from heparinized blood samples using Ficoll-Hypaque density gradient centrifugation (Sigma-Aldrich). PBMCs were cultured in RPMI-1640 medium (Gibco, Carlsbad, CA, USA) supplemented with 10% fetal bovine serum and stimulated overnight with lipopolysaccharide (LPS, 100 ng/mL; Solarbio, Hangzhou, China). EFC was applied to PBMCs at the same concentrations and durations as those used for RA FLSs.

THP-1 monocytes, sourced from BNCC (Henan, China), were differentiated into M1 macrophages by treating them with 200 nM phorbol-12-myristate-13-acetate (Sigma-Aldrich, St. Louis, MO) for 24 h, followed by stimulation with LPS (250 ng/mL) and interferon-γ (20 ng/mL; PeproTech, NJ, USA) for an additional 48 h.[19] Subsequently, M1 macrophages were treated with EFC using the same concentrations and incubation periods as those applied to RA FLSs.

Cell Counting Kit-8 (CCK-8) assay

Cells were seeded into 96-well plates at a density of 3 × 10^4 cells per well, then treated with the specified concentrations of EFC and methotrexate. Following treatment, 10 μL of CCK-8 reagent (Solarbio, Hangzhou, China) was added to each well, and the plates were incubated for 1 h. The absorbance was recorded at 450 nm with a microplate reader (SpectraMax ID3, Molecular Devices, Silicon Valley, USA).

EdU assay

The EdU proliferation assay was carried out as previously described.[20] In brief, 1 × 10^4 cells were seeded onto 24-well plates and subsequently treated for 24 h with EFC at 1 μM and 2 μM, as well as methotrexate (10 μM). EdU staining was performed using the EdU DNA Cell Proliferation Kit (RiboBio, Guangzhou, China). Cells were treated with EdU (1:1,000) for 10 h, then fixed with paraformaldehyde and permeabilized with PBS containing 0.3% Triton X-100 for 10 m. The cells were then stained in the dark for 30 m with Apollo staining solution, followed by 5 m of DAPI staining to allow for visibility with an Olympus fluorescent microscope (Olympus Culture Microscopes, Center Valley, PA, USA).

Real-time polymerase chain reaction (PCR)

Total RNA was isolated using Trizol reagent (Vazyme, Nanjing, China), with RNA purity values ranging from 1.8 to 2.0. Complementary DNA (cDNA) was synthesized from 1 μg of RNA employing the THUNDERBIRD® Next SYBR quantitative PCR (qPCR) mixture (TOYOBO, Japan). Real-time quantitative PCR was conducted using the SYBR Green Mastermix kit (Cwbio, Jiangsu, China) on a Roche 480 instrument (Basel, Switzerland). Primer sequences used are provided in Table 1.

Migration, invasion, and angiogenesis experiment

Transwell chambers (Corning, Corning, USA) were used according to the manufacturer's protocol. 1 × 10^4 cells were resuspended in 200 μL media with 1% serum and placed in the top chamber. 500 μL of full culture medium was added to the lower chamber. The system was then incubated for 14 h at 37°C. Subsequently, the cells were fixed in 4% paraformaldehyde for 30 m before being stained with 0.1% crystal violet for 20 m. Non-invaded cells were scraped from the membrane's upper surface using a cotton swab, and migratory cells were counted. For the invasion assay, Matrigel

Table 1. The sequence of primers used in this study

Gene	Forward	Reverse
Homo-GAPDH	ACCCAGAAGACTGTGGATGC	TTCAGCTCAGGGATGACCTT
Homo-IL-8	ACTGAGAGTGATTGAGAGTGGAC	AACCCTCTGCACCCAGTTTTC
Homo-IL-6	ACTCACCTCTTCAGAACGAATTG	CCATCTTTGGAAGGTTCAGGTTG
Homo-MMP-1	GGGGAGATCATCGGACAACTC	AGAATGGCCGAGTTCATGAGCT
Homo-VEGF	AGGGCAGAATCATCACGAAGT	AGGGTCTCGATTGGATGGCA
Homo-COX_2	TCAAGTCCCTGAGCATCTACGGTT	CTGTTGTGTGTGTGTCCCGCAGCCAGAT
Homo-iNOS	TTCAGTATCACAACCTCAGCAAG	TGGACCTGCAAGTTAAAATCCC
Homo-DDIT-3	GGAAACAGAGTGGTCATTCCC	CTGCTTGAGCCGTTCATTCTC
Homo-IGF-1	GCTCTTCAGTTCGTGTGTGGA	GCCTCCTTAGATCACAGCTCC
Homo-FGFR-3	TGCGTCGTGGAGAACAAGTTT	GCACGGTAACGTAGGGTGTG
Homo-HMOX-1	AAGACTGCGTTCCTGCTCAAC	AAAGCCCTACAGCAACTGTCG
Homo-MAPK-14	TCAGTCCATCATTCATGCGAAA	AACGTCCAACAGACCAATCAC
Homo- ATF-3	CCTCTGCGCTGGAATCAGTC	TTCTTTCTCGTCGCCTCTTTTT

(BD, USA) diluted in DMEM at a 1:8 ratio was used to uniformly coat the inner surface of the chamber. Staining was performed 16 h post-invasion.

Human umbilical vein endothelial cells (HUVECs) were seeded at a density of 1×10^5 cells per well to analyze tube development. After 4 h of incubation, tube development was examined under a microscope.

Western blot

Total cellular proteins were extracted with RIPA lysis buffer (Beyotime, Shanghai, China) and heated at 95°C for 5 m. Protein samples (10 μg) were separated using sodium dodecyl sulfate-polyacrylamide gel electrophoresis (SDS-PAGE) and subsequently transferred to PVDF membranes (Merck, Shanghai, China). After blocking the membranes for 1 h with 5% skim milk powder, the corresponding primary antibody was incubated overnight at 4°C. The antibodies used in the present study were as follows: Bax (21 kDa, ET1603-34, 1:1,000, HUABIO, Hangzhou, China), Bcl-2 (26 kDa, 1:1,000, HUABIO, Hangzhou, China), Caspase-3 (32 kDa, ET1603-26, 1:1,000, HUABIO, Hangzhou, China), Cleaved Caspase-3 (17 kDa, ab2302, 1:1,000, Abcam, Cambridge, USA), Akt (60 kDa, CST#9272, 1:1,000, CST, Danvers, MA, USA), P-Akt (60 kDa, CST#4060, 1:2,000, CST, Danvers, MA, USA), p65 (65 kDa, CST#3031, 1:1,000, CST, Danvers, MA, USA), P-p65 (65 kDa, CST#3033, 1:1,000, CST, Danvers, MA, USA), Erk1/2 (42/44 kDa, CST#9194, 1:1,000, CST, Danvers, MA, USA), P-Erk1/2 (42/44 kDa, CST#9101, 1:1,000, CST, Danvers, MA, USA), and GAPDH (36 kDa, Abcam, Cambridge, USA). HRP-coupled anti-rabbit IgG (ZB-230, 1:5,000, ZSGB-BIO, Beijing, China) or HRP-coupled antibody against mouse IgG (ZB-2306, 1:5,000, ZSGB-BIO, Beijing, China) were used as secondary antibodies.

Flow cytometry

Apoptosis was measured using a fluorescein isothiocyanate-Annexin V and propidium iodide detection kit from Bestbio (Shanghai, China). The cells were first treated with Annexin V binding buffer for 10 m, then incubated with fluorescein isothiocyanate-Annexin V for 5 m before being stained with propidium iodide. Flow cytometry analysis was performed using a FACSCalibur device (BD, New Jersey, USA) to measure the number of apoptotic cells.

TUNEL assay

Apoptosis was measured using the TUNEL test kit (Beyotime, China). The experiment was performed according to the manufacturer's instructions. Cells were first fixed in 4% paraformaldehyde for 10 m, then permeabilized with 0.3% Triton X-100 for 5 m. The cells were then treated with the TUNEL reaction mixture for 1 h at 37°C, followed by 5 m of DAPI counterstaining. Fluorescence signals from the TUNEL assay were visualized using an Olympus fluorescence microscope.

ELISA

Inflammatory cytokines were quantified using an ELISA kit (R&D Systems, Minneapolis, USA). Samples were added to the wells and incubated with an HRP-conjugated antibody at 37°C for 2 h while shaking at 200 RPM. After incubation, the plates were washed, and the enzyme-substrate reaction was initiated by adding the chromogenic substrate. Absorbance was measured using dual-wavelength analysis to determine cytokine concentrations.

Collagen-induced arthritis (CIA) model

Eight-week-old DBA mice (Cyagen Biosciences, Suzhou, China) were injected subcutaneously with 100 mg of Freund's complete adjuvant (Biosharp, Anhui, China), emulsified with bovine type II collagen (Chondrex, Washington, USA). On day 21, a secondary subcutaneous injection of 100 mg of bovine type II collagen emulsified with Freund's incomplete adjuvant (Biosharp, Anhui, China) was given.[21] Every three days for two weeks after injection, hind paw thickness and arthritis scores were measured. The scoring standards were similar to those of earlier research.[22,23] Based on their arthritis scores, the mice were randomly divided into two groups of nine. The first group received EFC injections, while the other group was treated with DMSO as a vehicle control. The study protocol was approved by the Medical Ethics Committee of the Institutional Review Board of Shandong Medical and Biotechnology Center (SMBC2020-07) and Shandong Province's Animal Care Committee. Informed consent for clinical research was obtained accordingly.

Hematoxylin-eosin (H&E) staining

The knee and elbow joints of mice were fixed for 24 h and subsequently decalcified using a 10% EDTA solution. The decalcification solution was replaced every three days over a period of 30 days. After decalcification, the tissues were fixed in paraffin and sectioned. H&E staining was performed on 5 μm slices of the knee, while Safranin-O and Fast Green staining were used to evaluate cartilage injury.

Microcomputed tomography scanning

Following four weeks of EFC administration, elbow and knee joints, as well as anterior and posterior paw tissues, were harvested. Bone destruction was assessed using microcomputed tomography. The scanning parameters were as follows: X-ray voltage: 90 kV; X-ray current: 88 μA; scanning duration: 14 m; field of view: 18 mm; pixel size: 36.0 μm. A total of 512 slices were analyzed for bone microarchitecture. Parameters for trabecular bone analysis of the tibia included trabecular separation (Tb.Sp, mm), relative trabecular bone volume (BV/TV, %), trabecular thickness (Tb.Th, mm), and trabecular bone mineral density (Tb.BMD, g/cm^3).

Statistical analysis

Data are presented as mean ± standard deviation (SD). The Mann–Whitney U-test was used for analysis of arthritis and paw swelling. GraphPad Prism 8.0 (GraphPad Software, San Diego, CA, USA) was used to evaluate the statistical significance of the differences. Other outcomes were evaluated using variance analysis (one-way ANOVA). A value of <0.05 was considered significant.

Results

RA FLSs were more sensitive to EFC

RA pathogenesis involves a variety of cell types, including FLSs, macrophages, and lymphocytes.[22] In this study, we initially evaluated cell viability using the CCK-8 assay after treating RA FLSs, PBMCs, and THP-1 cells with a range of EFC concentrations. As illustrated in Figure 1a, EFC demonstrated cytotoxic effects on all examined cell types at micromolar concentrations. Cell viability decreased in a dose-dependent manner within the 1–20 μM range. Specifically, EFC concentrations of 1–2 μM inhibited cell proliferation in a concentration-dependent manner without causing significant toxicity, indicating that these concentrations were optimal for subsequent experiments. EFC exhibited the greatest cytotoxicity toward RA FLSs (IC50 = 4.251 μM) compared to PBMCs (IC50 = 9.164 μM) and THP-1 cells (IC50 = 6.106 μM). Moreover, at lower concentrations (1 μM and 2 μM), EFC showed a more pronounced anti-inflammatory effect on RA FLSs (Fig. 1b). During RA progression, RA FLSs exhibit heightened sensitivity to stimuli such as hypoxia and metabolic dysfunction, which can promote ER stress and increase the expression of PDI family members, notably TXNDC5.[23] This increased sensitivity to EFC in RA FLSs, evidenced by the lowest IC50 value, suggests greater uptake and stronger binding affinity of EFC in these cells. Therefore, RA FLSs were selected for further pharmacological investigations.

EFC inhibited the inflammatory activity of RA FLSs

RA FLSs are crucial contributors to joint inflammation in RA, and targeting their activity represents an effective strategy to mitigate progressive inflammation in affected joints.[24] Once activated, RA FLSs secrete elevated levels of cytokines, chemokines, and matrix metalloproteinases, leading to synovial hyperplasia, pannus development, and subsequent bone and cartilage degradation.[24–26] As illustrated in Figure 2a, treatment with EFC over specified durations inhibited RA FLS proliferation in a dose-dependent manner. Additionally, EdU assay results showed that EFC significantly reduced the cell proliferation induced by IL-1β (Fig. 2b). Consistent findings from qPCR analysis demonstrated that EFC suppressed the expression of matrix metalloproteinase-1 and vascular endothelial growth factor (Fig. 2c). The inflammatory phenotype of RA FLSs is characterized by increased migration, invasion, and pro-angiogenic capabilities.[27–29] As expected, the number of RA FLSs undergoing migration and invasion in response to inflammatory stimuli significantly increased, but this trend was markedly attenuated by EFC in a dose-dependent manner (Fig. 2d, e). The anti-angiogenic activity of EFC was further evaluated using a tube formation assay with HUVECs. As shown in Figure 2f, the supernatants collected from EFC-treated RA FLSs inhibited HUVEC tube formation. Collectively, these findings suggest that EFC effectively suppresses the inflammatory activity of RA FLSs.

EFC promoted apoptosis of RA FLSs

Previous research has demonstrated that synovial hyperplasia is linked to the resistance of RA FLSs to apoptosis.[30] Inflammatory cytokines and hypoxic conditions trigger ER stress, subsequently activating the unfolded protein response (UPR). Activation of the UPR decreases the levels of pro-apoptotic proteins while increasing anti-apoptotic proteins, ultimately contributing to apoptotic resistance in RA FLSs.[31] TUNEL staining and flow cytometry analysis indicated that inflammatory stimuli reduced the number of apoptotic cells, whereas treatment with EFC (1 μM and 2 μM) increased apoptosis in a dose-dependent manner (Fig. 3a, b). To further investigate this mechanism, we assessed the expression of pro-apoptotic proteins Caspase-3 and Bax, as well as the anti-apoptotic protein Bcl-2. EFC treatment enhanced the expression of cleaved Caspase-3 and Bax while reducing Bcl-2 expression. These results indicate that EFC effectively overcomes the apoptotic resistance of RA FLSs (Fig. 3c).

EFC mitigates disease progression in CIA mice

The type II collagen-induced CIA model exhibits similar pathogenesis and clinical manifestations to RA, making it a widely used model for investigating the pathological mechanisms and evaluating drug efficacy in RA.[32] To assess the safety of EFC, healthy DBA mice were given 10 mg/kg intraperitoneally for 14 consecutive days. Routine hematological and biochemical measures did not show any significant changes compared to controls.

In the CIA model, EFC was administered intraperitoneally at a dose of 5 mg/kg from day 22 to day 49 post-initial immunization. The treatment significantly reduced arthritis scores (Fig. 4a) and paw swelling in the CIA mice (Fig 4b, c). To investigate whether EFC could decrease systemic inflammatory cytokine production, serum levels of inflammatory markers were measured. CIA animals showed significantly higher levels of IL-6, IL-8, IL-1α, and TNF-α compared to healthy DBA control mice. Notably, EFC treatment significantly attenuated these increases (Fig. 4d).

To determine whether EFC ameliorates synovial hyperplasia, knee joint sections from CIA mice were stained with H&E. EFC treatment clearly reduced synovial hyperplasia, inflammatory cell infiltration, and pannus development in the CIA model (Fig. 4e). Following Safranin-O staining, it was evident that EFC treatment significantly mitigated cartilage destruction (Fig. 4f). Furthermore, bone parameters such as trabecular bone mineral density

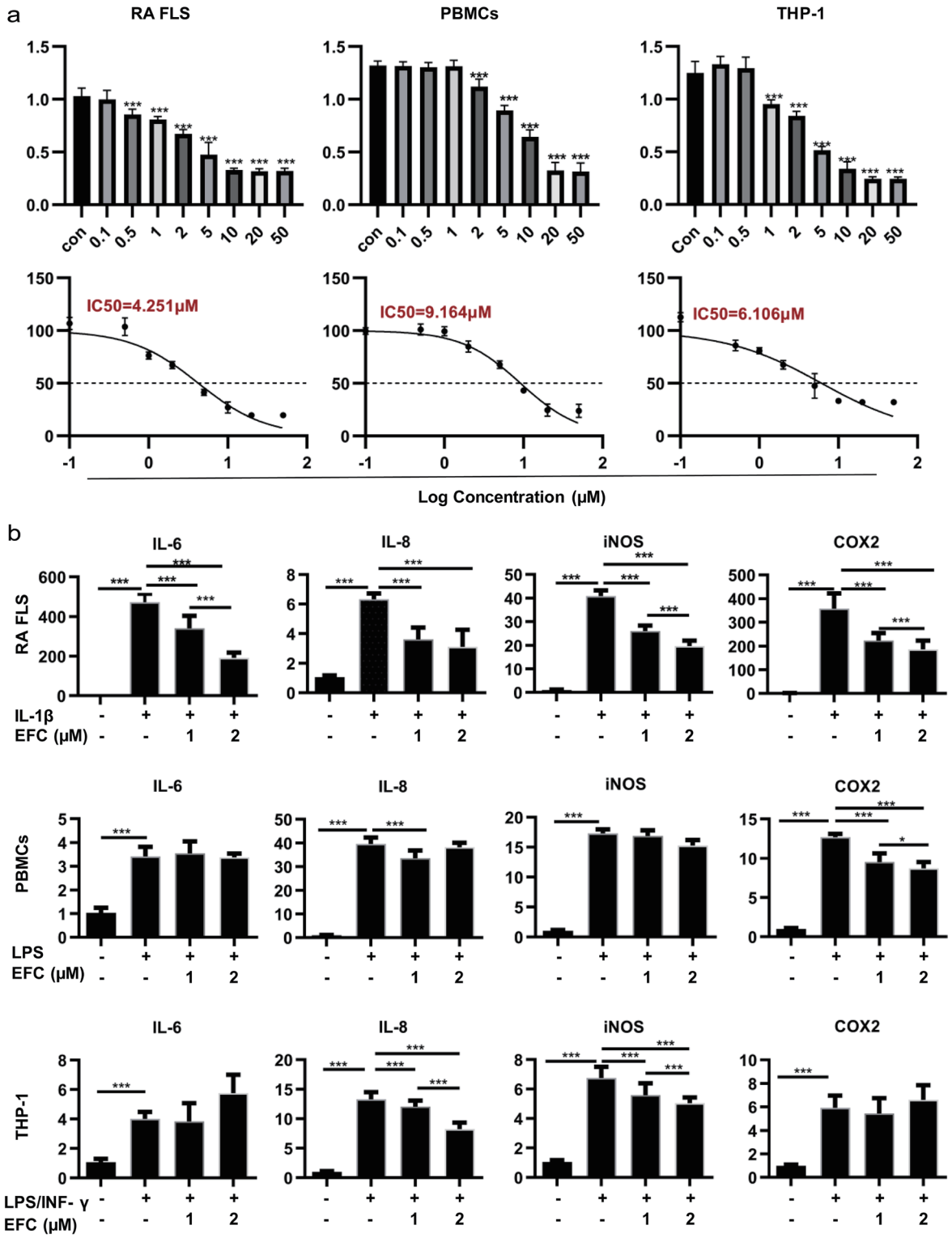

Fig. 1. The effects of EFC on RA FLSs, PBMCs, and THP-1 cells. RA FLSs, PBMCs, and THP-1 cells were treated with vehicle control and different concentrations of EFC for 72 h (a) or 24 h (b). (a) The cell number was measured using the CCK-8 assay, and IC50 values were derived. (b) Total RNA was collected, and the mRNA levels of IL-6, IL-8, NOS2, and COX2 were measured by RT-qPCR. Data are presented as mean ± standard deviation (SD). $^{**}p < 0.01$, $^{***}p < 0.001$. CCK-8, Cell Counting Kit-8; COX, cyclooxygenase; EFC, E64FC26; FLSs, fibroblast-like synoviocytes; IC50, inhibitory concentration 50; IL, interleukin; IFN-γ, Interferon-gamma; LPS, lipopolysaccharide; NOS, nitric oxide synthase; PBMCs, peripheral blood mononuclear cells; RA, rheumatoid arthritis; RT-qPCR, real-time quantitative polymerase chain reaction; THP-1, human monocytic leukemia cell line.

 DOI: 10.14218/ERHM.2024.00033 | Volume 10 Issue 1, January 2025

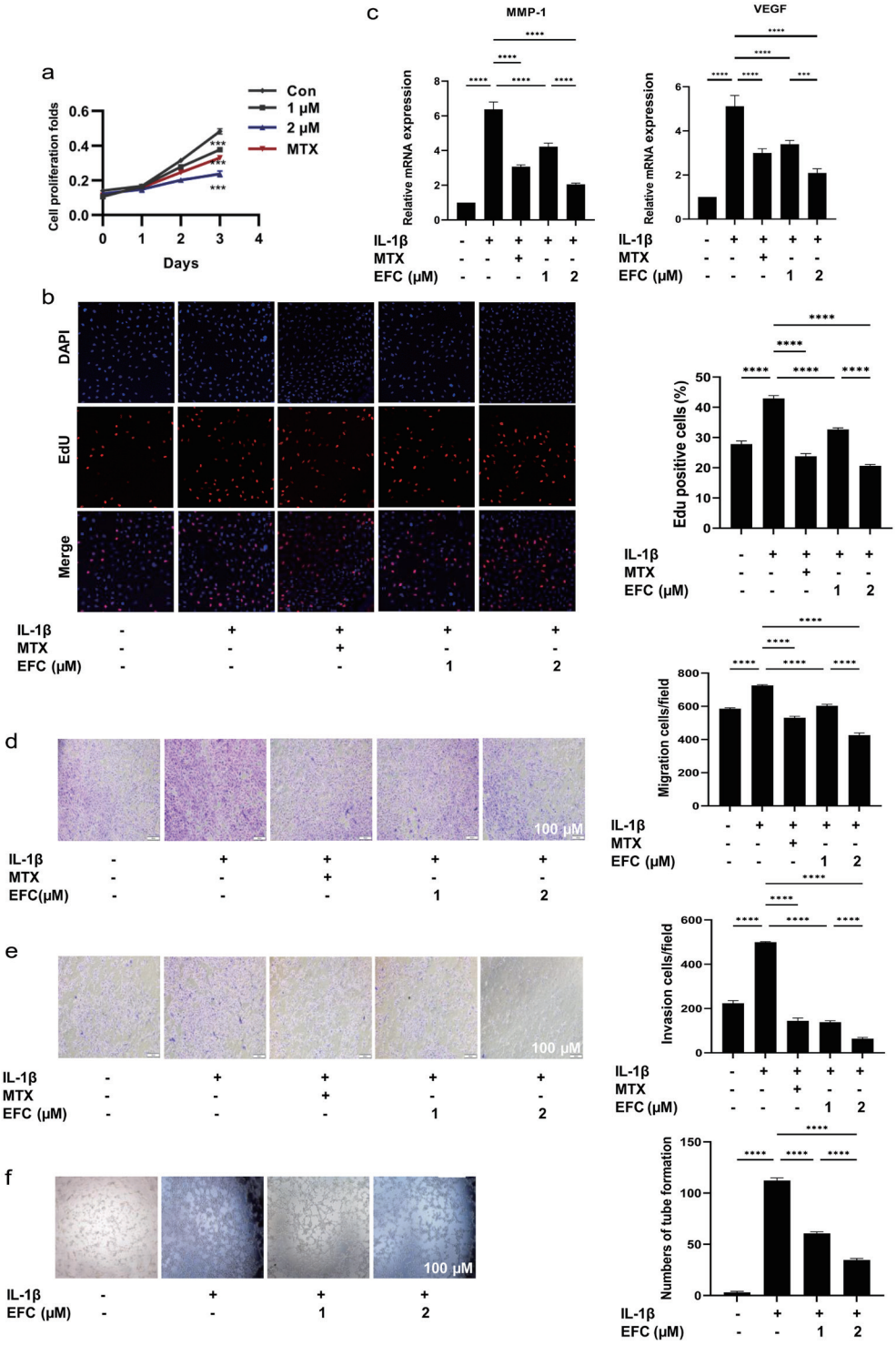

Fig. 2. Effect of EFC on the bioactivity of RA FLSs. (a) In the presence of IL-1β, RA FLSs were treated with EFC (1 μM, 2 μM) for the indicated time periods. MTX was used as a positive control group (10 μM). The CCK-8 assay was used to detect cell viability. (b-f). RA FLSs were pretreated with EFC or MTX for 24 h, followed by treatment with IL-1β or PBS. Cell proliferation, migration, and invasion were assessed using the EdU test (b), Transwell migration assay (d), and Transwell Matrigel invasion assay (e). (c) The expression levels of MMP-1 and VEGF were measured by RT-qPCR. (f) The culture supernatants of RA FLSs with indicated treatment were collected for culturing with HUVEC to perform a tube formation assay. Data are presented as mean ± standard deviation (SD). *$p < 0.05$, **$p < 0.01$, ***$p < 0.001$, ****$p < 0.0001$. CCK-8, Cell Counting Kit-8; EFC, E64FC26; IL, interleukin; MTX, methotrexate; RA, rheumatoid arthritis; FLSs, fibroblast-like synoviocytes; RT-qPCR, real-time quantitative polymerase chain reaction; PBS, phosphate buffered saline; MMP-1, matrix metalloproteinase-1; VEGF, vascular endothelial growth factor; HUVEC, human umbilical vein endothelial cells.

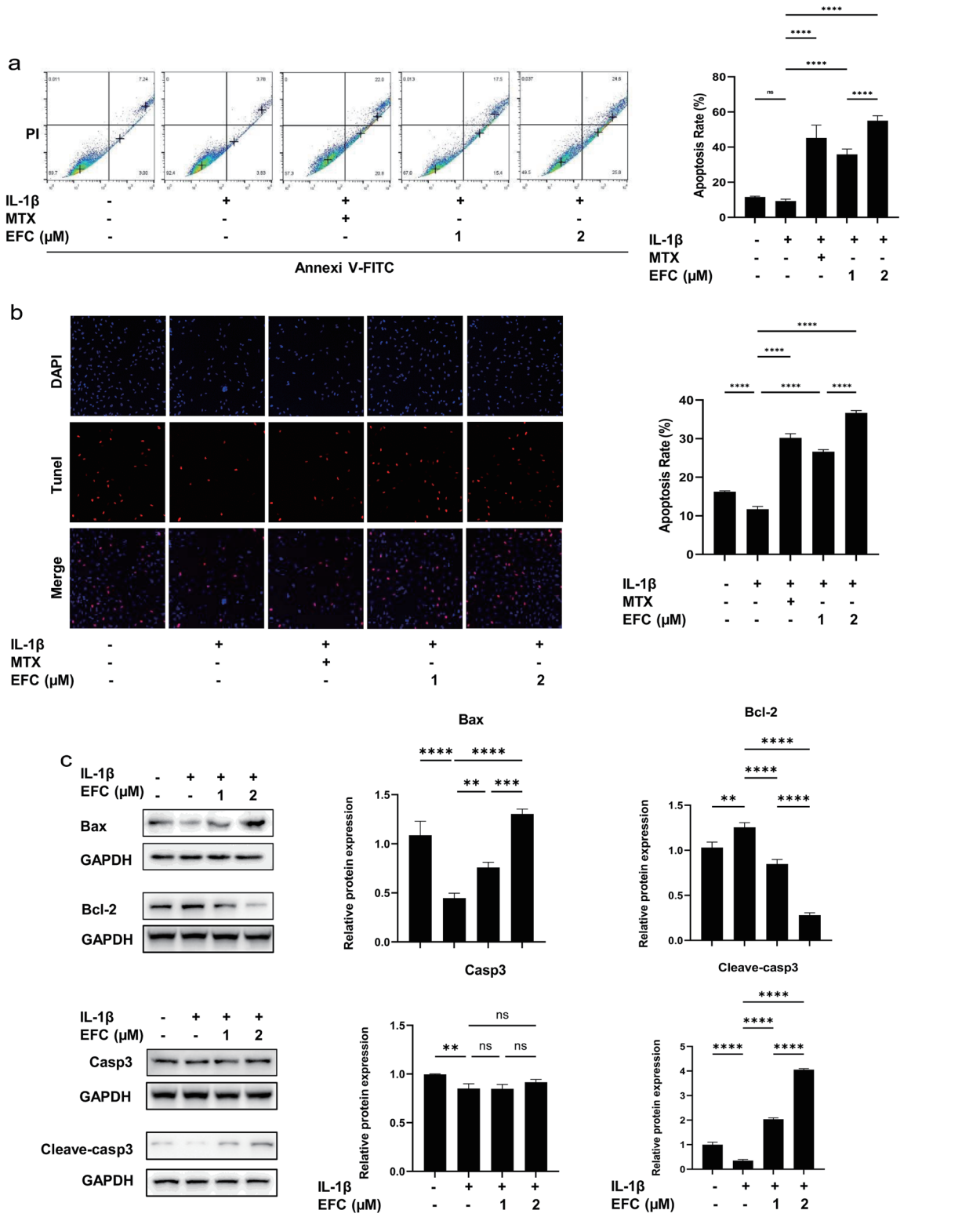

Fig. 3. EFC promotes apoptosis of RA FLSs. In response to the activation of IL-1β, RA FLSs were treated with EFC (1 μM, 2 μM), MTX (10 μM), or vehicle for 24 h. The proportion of apoptotic cells was evaluated by flow cytometry (a) and TUNEL assay (b), with flow cytometry using Alexa Fluor 488 Annexin V/PI. (c) Total proteins were extracted, and the expression of apoptosis-related proteins was detected by Western blot. Data are presented as mean ± standard deviation (SD). *$p < 0.05$, **$p < 0.01$, ***$p < 0.001$, ****$p < 0.0001$. EFC, E64FC26; FLSs, fibroblast-like synoviocytes; IL, interleukin; MTX, methotrexate; RA, rheumatoid arthritis; PI, propidium iodide.

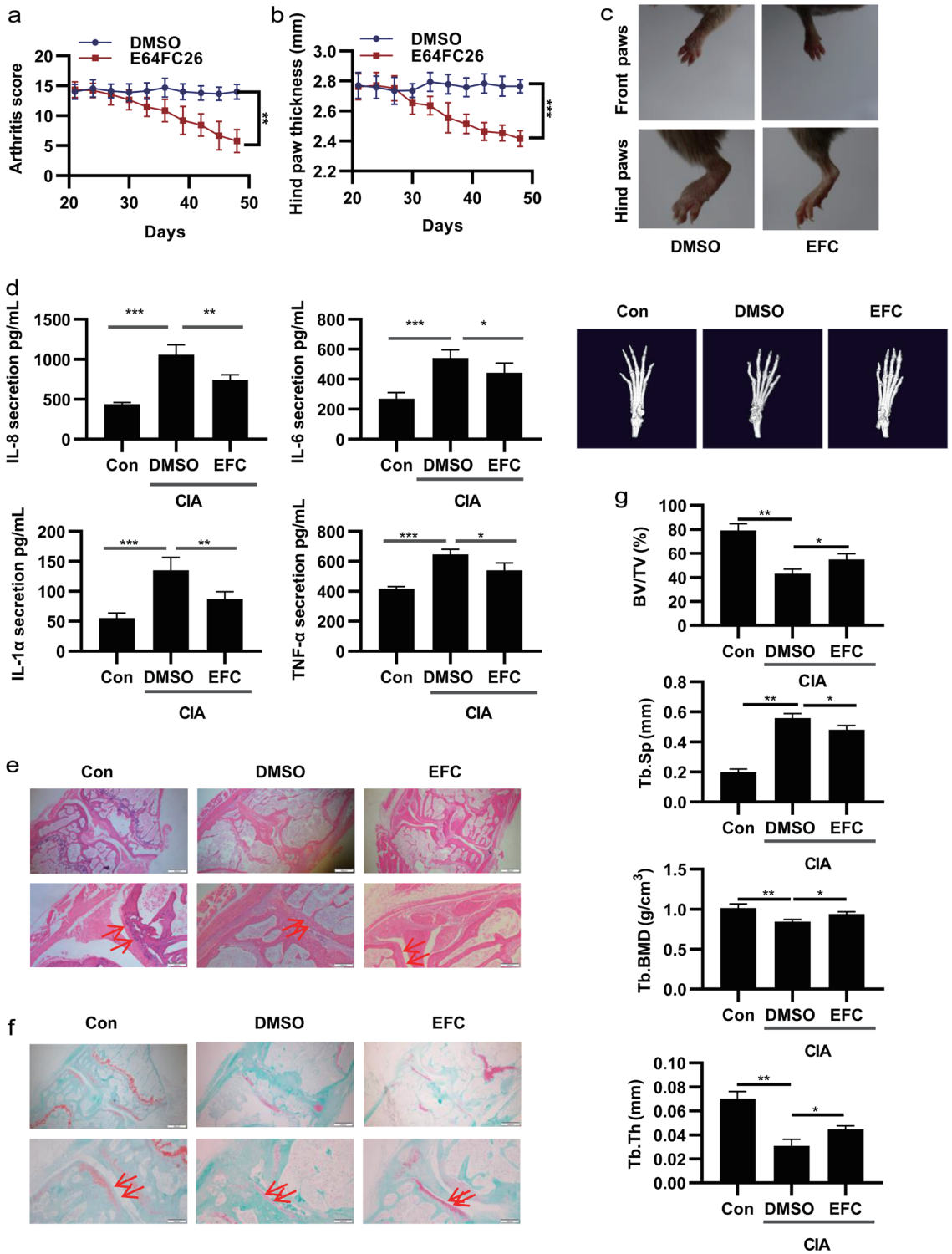

Fig. 4. EFC mitigates disease progression in CIA models. From days 22 to 49, CIA mice received intraperitoneal injections of 5 mg/kg EFC three times per week. (a) Arthritis score was assessed every three days. (b) Paw thickness was measured by caliper every three days. (c) Paw was photographed on day 49. (d) The blood levels of TNF-α, IL-6, IL-8, and IL-1α were evaluated using an ELISA test. (e, f) Knee joint slices were stained with hematoxylin and eosin (original magnification, 40× and 100×) and Safranin O (original magnification, 200×). Histological inflammation scores are displayed (n = 3). (g) Microcomputed tomography was used to assess bone microstructure. Data are presented as mean ± standard deviation (SD). *$p < 0.05$, **$p < 0.01$, ***$p < 0.001$, ****$p < 0.0001$. CIA, collagen-induced arthritis; EFC, E64FC26; IL, interleukin; TNF, tumor necrosis factor; RA, rheumatoid arthritis; FLSs, fibroblast-like synoviocytes; ELISA, enzyme-linked immunosorbent assay.

(Tb.BMD), bone volume fraction (BV/TV%), trabecular number (Tb.N), and trabecular thickness (Tb.Th) were considerably lower in CIA mice than in healthy controls, while trabecular separation (Tb.Sp) increased. However, these parameters were restored with EFC treatment (Fig. 4g).

Overall, these findings indicate that EFC effectively inhibits the progression of CIA.

RNA-Seq analysis

A transcriptional analysis was performed to investigate the molecular mechanisms underlying EFC. Figure 5a shows that EFC increased the expression of 373 genes while decreasing the expression of 323 genes in RA FLSs. KEGG pathway analysis revealed that differentially expressed genes (DEGs) were primarily involved in pathways such as cytokine-cytokine receptor interaction, MAPK, and Ras signaling, all of which are strongly related to the inflammatory and apoptosis-resistant characteristics of RA FLSs (Fig. 5b). Further analysis identified that 105 of these DEGs were associated with both inflammation and apoptosis (Fig. 5c).[24,33,34] The potential interactions among these 105 DEGs were examined using the STRING database, revealing extensive and strong associations between them (Fig. 5d). To confirm the reliability of the RNA-seq data, qPCR validation was conducted, showing consistent DEG expression with the sequencing results (Fig. 5e, f).

To determine whether the differential sensitivity of EFC in RA FLSs, PBMCs, and THP-1 cells is pathway-dependent, we focused on TXNDC5, a member of the PDI family known to facilitate RA progression through activation of NF-κB signaling.[35] The RNA sequencing results indicated activation of the Ras and MAPK pathways in response to EFC. Therefore, we assessed the phosphorylation status of AKT, p65, and ERK1/2 following EFC treatment. EFC effectively inhibited the phosphorylation of AKT, p65, and ERK1/2, with the inhibitory effects being more pronounced in RA FLSs compared to PBMCs and THP-1 cells (Fig. 5g).

Discussion

This study examines the therapeutic potential of EFC for RA treatment using extensively *in vitro* and *in vivo* tests. The findings highlight the impact of EFC on RA FLSs as well as its overall anti-inflammatory benefits in a CIA paradigm. Despite the efficacy of current RA therapies, such as disease-modifying antirheumatic drugs and biologics targeting TNF and IL-6, a subset of patients—particularly those classified as difficult-to-treat—fail to achieve remission due to limited treatment options and poor adherence.[36–39] As a result, there is an urgent need for innovative therapies that target different mechanisms. EFC presents a promising approach by affecting cellular pathways involved in RA FLS proliferation, inflammation, and resistance to apoptosis.

The over-proliferation and migration of RA FLSs are critical contributors to synovial hyperplasia and joint damage in RA. Our results show that EFC significantly inhibits RA FLS proliferation and migration at micromolar concentrations, with a more pronounced effect on RA FLSs compared to PBMCs and THP-1 cells. Previous studies underscore the role of cytokine signaling in promoting RA FLS proliferation and inflammation.[40] In our study, EFC treatment significantly downregulated inflammatory cytokines IL-6, IL-8, iNOS, and COX-2, suggesting that EFC reduces RA-associated inflammation by attenuating these cytokine pathways, thereby limiting RA FLS activity and disease progression.

RA pathology is characterized by an aberrant UPR in RA FLSs, which promotes apoptosis resistance and contributes to chronic inflammation.[41,42] Our findings indicate that EFC effectively induces apoptosis in RA FLSs by increasing the levels of pro-apoptotic proteins (Caspase-3, Bax) and decreasing the expression of the anti-apoptotic protein Bcl-2. This suggests that EFC may counteract the apoptosis resistance observed in RA, supporting the strategy of UPR inhibition to enhance synoviocyte apoptosis. By disrupting the UPR pathway, EFC shows potential as a targeted agent to promote RA FLS apoptosis and mitigate synovial hyperplasia.

In the CIA mouse model, EFC was effective in reducing RA-associated inflammation and joint destruction while maintaining a favorable safety profile. EFC treatment significantly decreased levels of inflammatory cytokines, including IL-6, IL-8, IL-1β, and TNF-α. These *in vivo* findings align with *in vitro* observations, demonstrating that EFC not only acts at the cellular level but also confers organism-wide therapeutic benefits, reducing synovial inflammation and preserving joint integrity. This validates EFC's potential as an anti-inflammatory drug for RA treatment.

Gene expression analysis revealed that EFC influences key pathways involved in RA pathology, particularly those related to cytokine-receptor interactions and MAPK and Ras signaling pathways, which are crucial for RA FLS proliferation and resistance to apoptosis.[43] EFC inhibited the phosphorylation of AKT and ERK1/2, suggesting interference with RA FLS survival mechanisms and further supporting its potential to mitigate RA FLS overactivity. This modulation of signaling pathways provides valuable insight into EFC's mechanisms of action, reinforcing its relevance to RA treatment strategies targeting inflammation and cell survival at the molecular level.

Our results confirm the multifaceted therapeutic effects of EFC in RA treatment. Preliminary mechanistic analyses suggest that EFC disrupts both inflammatory and apoptosis-resistant signaling in RA FLSs. Future studies should focus on optimizing interactions between EFC and PDI family proteins to elucidate their roles in UPR regulation. Given the complexity of RA and variability in patient responses, evaluating EFC's efficacy in combination with current therapies and assessing its potential for clinical translation are crucial next steps. Such research could enhance the effectiveness and accessibility of RA treatments, particularly for difficult-to-treat patients.

Future directions

While the anti-arthritic effects of EFC in RA have been demonstrated through both *in vitro and in vivo* experiments, certain limitations remain. Specifically, the heterogeneity of PDI expression among RA patients and the identification of populations that would most benefit from EFC treatment have yet to be established. Additionally, it is unclear whether EFC could be effectively combined with existing therapies to enhance clinical outcomes in refractory cases. Consequently, further studies are required to evaluate EFC's therapeutic potential for RA. Investigating the binding affinity of EFC to PDIs, the number of binding sites, binding distance, and its influence on the spatial conformation of PDIs will provide more information on the mechanism of EFC action.[44–46] Future research will use techniques such as circular dichroism spectroscopy, differential scanning calorimetry, and time-resolved fluorescence analysis to further understand the molecular mechanisms and dynamics of EFC.[47]

Conclusions

Our study shows that EFC reduces the inflammatory phenotype of RA FLSs, significantly lowering inflammation and joint de-

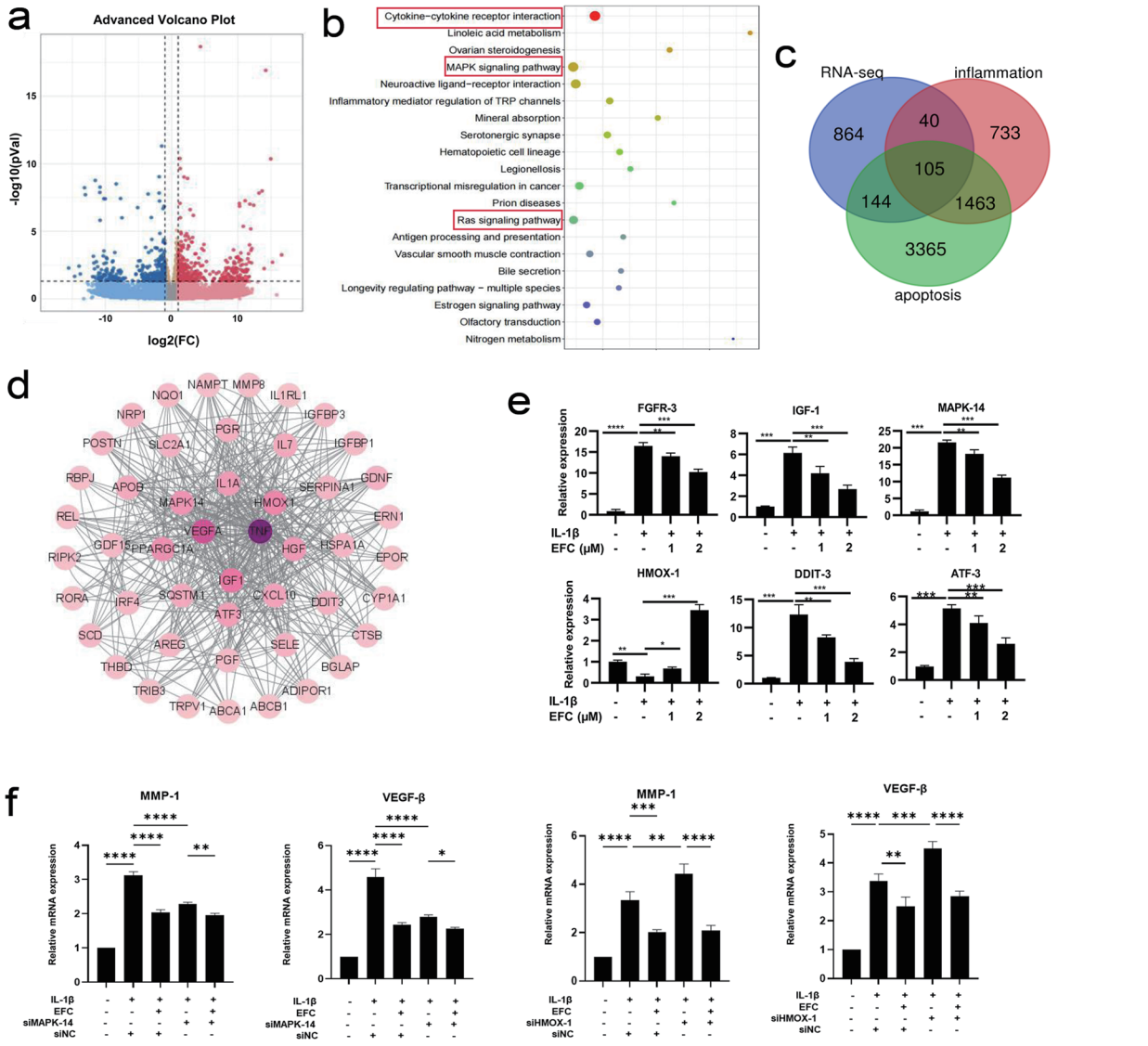

(continued)

Fig. 5. Potential pathways in EFC-treated RA FLSs predicted by RNA-seq analysis. (a, b) The Volcano plots and KEGG analysis of the differentially expressed genes. (c) Venn diagram comparison analysis between DEGs, apoptosis-related genes, and inflammation-related genes. (d) DEGs related to apoptosis and inflammation were added to the STRING database for analysis. (e) qPCR validation of differential gene expression. (f) Validation of RNA sequencing results: First, RA FLSs were activated with IL-1β for 6 h. Following that, the cells, with or without silenced HMOX-2 or MAPK-14, were treated with EFC or DMSO for another 24 h. RA FLSs were tested for MMP-1 and VEGF-β expression levels using quantitative PCR (qPCR). (g) The total protein was extracted, and the expressions of total and phosphorylated Akt, p65, and Erk1/2 were determined using Western blotting. Data are presented as mean ± standard deviation (SD). *$p < 0.05$, **$p < 0.01$, ***$p < 0.001$, ****$p < 0.0001$. DEG, differentially expressed gene; DMSO, dimethyl sulfoxide; EFC, E64FC26; FLSs, fibroblast-like synoviocytes; HMOX-2, heme oxygenase-2; IL, interleukin; KEGG, kyoto encyclopedia of genes and genomes; MAPK-14, mitogen-activated protein kinase-14; MMP-1, matrix metalloproteinase-1; qPCR, quantitative polymerase chain reaction; RA, rheumatoid arthritis; VEGF, vascular endothelial growth factor.

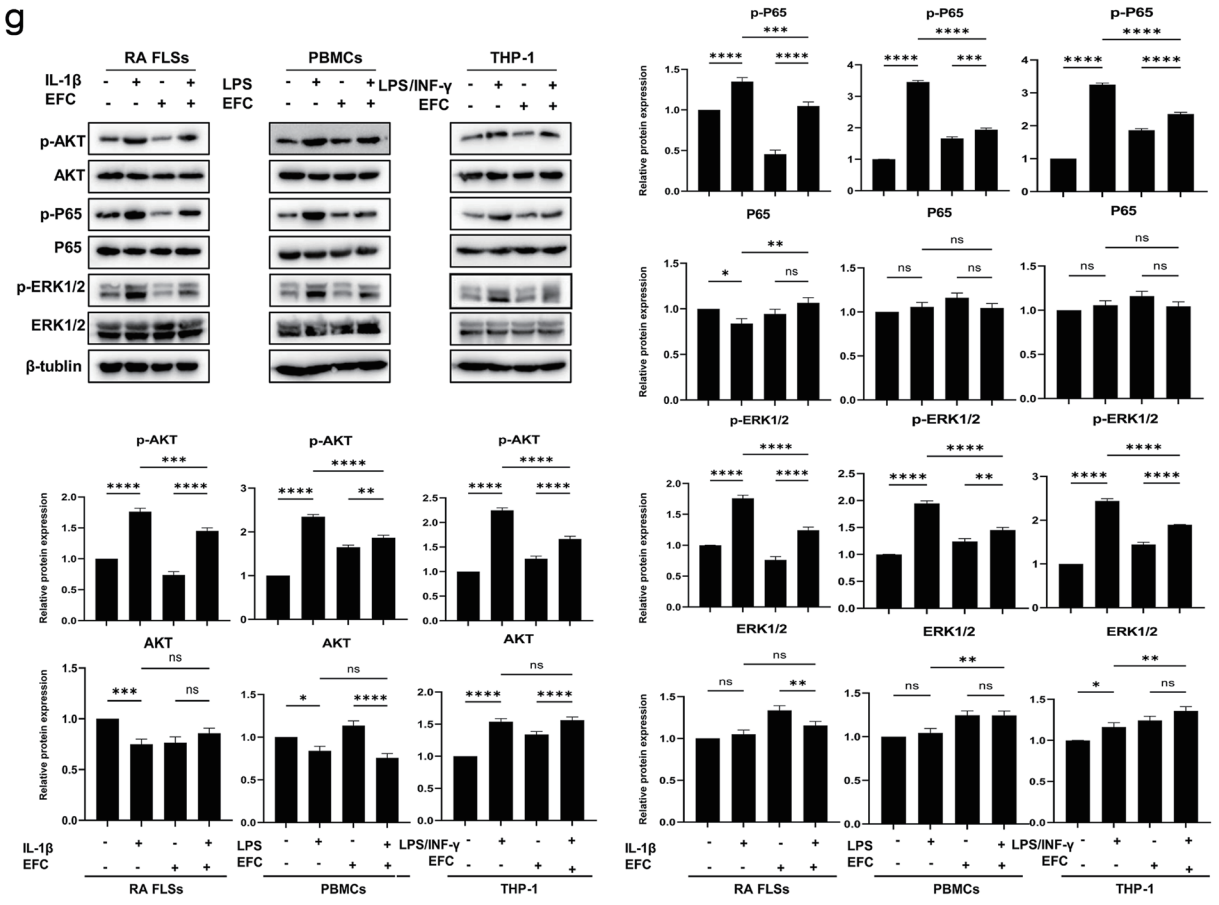

Fig. 5. *(continued)*

struction in animal arthritis models. These findings expand on the known functions of EFC, revealing its therapeutic potential for RA alongside its established anti-tumor properties. This highlights the need for lateral thinking, which may facilitate optimal utilization of existing treatments. Furthermore, our research confirms the role of PDIs in promoting RA, providing a foundation for the future application of PDIs as therapeutic targets in RA management.

Acknowledgments

We would like to thank the members of the laboratory for their assistance and support.

Funding

This work was supported by the National Natural Science Foundation of China (Grant No. 81772760, 82072850, 81901666, 82101903, 82171801), the Natural Science Foundation of Shandong Province (Grant No. ZR2020YQ55), the Key Research and Development Project of Shandong Province (No. 2021ZDSYS27), The Innovation Project of Shandong Academy of Medical Sciences (2021), The Youth Innovation Technology Plan of Shandong University (Grant No. 2019KJK003), the Academic Promotion Programme of Shandong First Medical University (Grant No. 2019LJ001), and Shandong Provincial Central Government Guide Local Science and Technology Development Fund Projects (YDZX20203700002055).

Conflict of interest

The authors declare no competing interests.

Author contributions

Contributed to study concept and design (JXH, LW), data acquisition (HYZ, TW, LNG, GHS), data analysis and interpretation (HYZ, RJZ, YAZ), manuscript drafting (LW, LNG), and critical revision for important intellectual content (JXH, JHP). All authors made significant contributions to this study and approved the final manuscript.

Ethical statement

All animal studies were approved by the Institutional Animal Care and Use Committee of Shandong First Medical University & Shandong Academy of Medical Sciences (SMBC21LL028).

Data sharing statement

The data that support the findings of this study are available from

the corresponding author upon reasonable request.

References

[1] Zhai KF, Duan H, Khan GJ, Xu H, Han FK, Cao WG, *et al*. Salicin from Alangium chinense Ameliorates Rheumatoid Arthritis by Modulating the Nrf2-HO-1-ROS Pathways. J Agric Food Chem 2018;66(24):6073–6082. doi:10.1021/acs.jafc.8b02241, PMID:29852739.

[2] Dai Y, Wang W, Yu Y, Hu S. Rheumatoid arthritis-associated interstitial lung disease: an overview of epidemiology, pathogenesis and management. Clin Rheumatol 2021;40(4):1211–1220. doi:10.1007/s10067-020-05320-z, PMID:32794076.

[3] Abbasi M, Mousavi MJ, Jamalzehi S, Alimohammadi R, Bezvan MH, Mohammadi H, *et al*. Strategies toward rheumatoid arthritis therapy; the old and the new. J Cell Physiol 2019;234(7):10018–10031. doi:10.1002/jcp.27860, PMID:30536757.

[4] Burmester GR, Pope JE. Novel treatment strategies in rheumatoid arthritis. Lancet 2017;389(10086):2338–2348. doi:10.1016/S0140-6736(17)31491-5, PMID:28612748.

[5] Fu XM, Zhu BT. Both PDI and PDIp can attack the native disulfide bonds in thermally-unfolded RNase and form stable disulfide-linked complexes. Biochim Biophys Acta 2011;1814(4):487–495. doi:10.1016/j.bbapap.2011.01.004, PMID:21238616.

[6] Hatahet F, Ruddock LW. Protein disulfide isomerase: a critical evaluation of its function in disulfide bond formation. Antioxid Redox Signal 2009;11(11):2807–2850. doi:10.1089/ars.2009.2466, PMID:19476414.

[7] Nie Q, Yang J, Zhou X, Li N, Zhang J. The Role of Protein Disulfide Isomerase Inhibitors in Cancer Therapy. ChemMedChem 2024;20(1):e202400590. doi:10.1002/cmdc.202400590, PMID:39319369.

[8] Lin CH, Tariq MJ, Ullah F, Sannareddy A, Khalid F, Abbas H, *et al*. Current Novel Targeted Therapeutic Strategies in Multiple Myeloma. Int J Mol Sci 2024;25(11):6192. doi:10.3390/ijms25116192, PMID:38892379.

[9] Ye ZW, Zhang J, Aslam M, Blumental-Perry A, Tew KD, Townsend DM. Protein disulfide isomerase family mediated redox regulation in cancer. Adv Cancer Res 2023;160:83–106. doi:10.1016/bs.acr.2023.06.001, PMID:37704292.

[10] Hurst KE, Lawrence KA, Reyes Angeles L, Ye Z, Zhang J, Townsend DM, *et al*. Endoplasmic Reticulum Protein Disulfide Isomerase Shapes T Cell Efficacy for Adoptive Cellular Therapy of Tumors. Cells 2019;8(12):1514. doi:10.3390/cells8121514, PMID:31779147.

[11] Chang X, Cui Y, Zong M, Zhao Y, Yan X, Chen Y, *et al*. Identification of proteins with increased expression in rheumatoid arthritis synovial tissues. J Rheumatol 2009;36(5):872–880. doi:10.3899/jrheum.080939, PMID:19369474.

[12] Wang L, Dong H, Song G, Zhang R, Pan J, Han J. TXNDC5 synergizes with HSC70 to exacerbate the inflammatory phenotype of synovial fibroblasts in rheumatoid arthritis through NF-κB signaling. Cell Mol Immunol 2018;15(7):685–696. doi:10.1038/cmi.2017.20, PMID:28603283.

[13] Zheng W, Lu X, Fu Z, Zhang L, Li X, Xu X, *et al*. Identification of candidate synovial membrane biomarkers after Achyranthes aspera treatment for rheumatoid arthritis. Biochim Biophys Acta 2016;1864(3):308–316. doi:10.1016/j.bbapap.2015.12.010, PMID:26724776.

[14] Wang L, Dong H, Song G, Zhang R, Pan J, Han J. TXNDC5 synergizes with HSC70 to exacerbate the inflammatory phenotype of synovial fibroblasts in rheumatoid arthritis through NF-κB signaling. Cell Mol Immunol 2018;15(7):685–696. doi:10.1038/cmi.2017.20, PMID:28603283.

[15] Yang CL, Wang FX, Luo JH, Rong SJ, Lu WY, Chen QJ, *et al*. PDIA3 orchestrates effector T cell program by serving as a chaperone to facilitate the non-canonical nuclear import of STAT1 and PKM2. Mol Ther 2024;32(8):2778–2797. doi:10.1016/j.ymthe.2024.05.038, PMID:38822524.

[16] Harrison BJ, Symmons DP, Barrett EM, Silman AJ. The performance of the 1987 ARA classification criteria for rheumatoid arthritis in a population based cohort of patients with early inflammatory polyarthritis. American Rheumatism Association. J Rheumatol 1998;25(12):2324–2330. PMID:9858425.

[17] Ospelt C, Kurowska-Stolarska M, Neidhart M, Michel BA, Gay RE, Laufer S, *et al*. The dual inhibitor of lipoxygenase and cyclooxygenase ML3000 decreases the expression of CXCR3 ligands. Ann Rheum Dis 2008;67(4):524–529. doi:10.1136/ard.2007.071589, PMID:17666446.

[18] Zhai KF, Duan H, Khan GJ, Xu H, Han FK, Cao WG, *et al*. Salicin from Alangium chinense Ameliorates Rheumatoid Arthritis by Modulating the Nrf2-HO-1-ROS Pathways. J Agric Food Chem 2018;66(24):6073–6082. doi:10.1021/acs.jafc.8b02241, PMID:29852739.

[19] Zhai K, Duan H, Wang W, Zhao S, Khan GJ, Wang M, *et al*. Ginsenoside Rg1 ameliorates blood-brain barrier disruption and traumatic brain injury via attenuating macrophages derived exosomes miR-21 release. Acta Pharm Sin B 2021;11(11):3493–3507. doi:10.1016/j.apsb.2021.03.032, PMID:34900532.

[20] Jemal M, Rao S, Gatz M, Whigan D. Liquid chromatography-tandem mass spectrometric quantitative determination of the HIV protease inhibitor atazanavir (BMS-232632) in human peripheral blood mononuclear cells (PBMC): practical approaches to PBMC preparation and PBMC assay design for high-throughput analysis. J Chromatogr B Analyt Technol Biomed Life Sci 2003;795(2):273–289. doi:10.1016/s1570-0232(03)00589-0, PMID:14522032.

[21] Lin YJ, Anzaghe M, Schülke S. Update on the Pathomechanism, Diagnosis, and Treatment Options for Rheumatoid Arthritis. Cells 2020;9(4):880. doi:10.3390/cells9040880, PMID:32260219.

[22] Makuch S, Więcek K, Woźniak M. The Immunomodulatory and Anti-Inflammatory Effect of Curcumin on Immune Cell Populations, Cytokines, and In Vivo Models of Rheumatoid Arthritis. Pharmaceuticals (Basel) 2021;14(4):309. doi:10.3390/ph14040309, PMID:33915757.

[23] Chang X, Zhao Y, Yan X, Pan J, Fang K, Wang L. Investigating a pathogenic role for TXNDC5 in rheumatoid arthritis. Arthritis Res Ther 2011;13(4):R124. doi:10.1186/ar3429, PMID:21801346.

[24] Li L, Pan Z, Ning D, Fu Y. Rosmanol and Carnosol Synergistically Alleviate Rheumatoid Arthritis through Inhibiting TLR4/NF-κB/MAPK Pathway. Molecules 2021;27(1):78. doi:10.3390/molecules27010078, PMID:35011304.

[25] Chen Y, Li H, Zhang XL, Wang W, Rashed MMA, Duan H. Exploring the anti-skin inflammation substances and mechanism of Paeonia lactiflora Pall. Flower via network pharmacology-HPLC integration. Phytomedicine 2024;129:155565. doi:10.1016/j.phymed.2024.155565, PMID:38579646.

[26] Li X, Wang Y. Cinnamaldehyde Attenuates the Progression of Rheumatoid Arthritis through Down-Regulation of PI3K/AKT Signaling Pathway. Inflammation 2020;43(5):1729–1741.

[27] Buch MH, Eyre S, McGonagle D. Persistent inflammatory and non-inflammatory mechanisms in refractory rheumatoid arthritis. Nat Rev Rheumatol 2021;17(1):17–33. doi:10.1038/s41584-020-00541-7, PMID:33293696.

[28] Bustamante MF, Garcia-Carbonell R, Whisenant KD, Guma M. Fibroblast-like synoviocyte metabolism in the pathogenesis of rheumatoid arthritis. Arthritis Res Ther 2017;19(1):110. doi:10.1186/s13075-017-1303-3, PMID:28569176.

[29] Neumann E, Schwarz MC, Hasseli R, Hülser ML, Classen S, Sauerbier M, *et al*. Tetraspanin CD82 affects migration, attachment and invasion of rheumatoid arthritis synovial fibroblasts. Ann Rheum Dis 2018;77(11):1619–1626. doi:10.1136/annrheumdis-2018-212954, PMID:29980577.

[30] Taghadosi M, Adib M, Jamshidi A, Mahmoudi M, Farhadi E. The p53 status in rheumatoid arthritis with focus on fibroblast-like synoviocytes. Immunol Res 2021;69(3):225–238. doi:10.1007/s12026-021-09202-7, PMID:33983569.

[31] Rahmati M, Moosavi MA, McDermott MF. ER Stress: A Therapeutic Target in Rheumatoid Arthritis? Trends Pharmacol Sci 2018;39(7):610–623. doi:10.1016/j.tips.2018.03.010, PMID:29691058.

[32] Alabarse PVG, Lora PS, Silva JMS, Santo RCE, Freitas EC, de Oliveira MS, *et al*. Collagen-induced arthritis as an animal model of rheumatoid cachexia. J Cachexia Sarcopenia Muscle 2018;9(3):603–612. doi:10.1002/jcsm.12280, PMID:29575818.

[33] Feng FB, Qiu HY. Retraction notice to "Effects of Artesunate on chondrocyte proliferation, apoptosis and autophagy through the PI3K/

AKT/mTOR signaling pathway in rat models with rheumatoid arthritis" [Biomed. Pharmacother. 102 (2018) 1209-1220]. Biomed Pharmacother 2023;162:114550. doi:10.1016/j.biopha.2023.114550, PMID:36967365.

[34] Yang X, Chang Y, Wei W. Emerging role of targeting macrophages in rheumatoid arthritis: Focus on polarization, metabolism and apoptosis. Cell Prolif 2020;53(7):e12854. doi:10.1111/cpr.12854, PMID:32530555.

[35] Ilchovska DD, Barrow DM. An Overview of the NF-kB mechanism of pathophysiology in rheumatoid arthritis, investigation of the NF-kB ligand RANKL and related nutritional interventions. Autoimmun Rev 2021;20(2):102741. doi:10.1016/j.autrev.2020.102741, PMID: 33340772.

[36] Buch MH. Defining refractory rheumatoid arthritis. Ann Rheum Dis 2018;77(7):966–969. doi:10.1136/annrheumdis-2017-212862, PMID:29588276.

[37] Prasad P, Verma S, Surbhi, Ganguly NK, Chaturvedi V, Mittal SA. Rheumatoid arthritis: advances in treatment strategies. Mol Cell Biochem 2023;478(1):69–88. doi:10.1007/s11010-022-04492-3, PMID: 35725992.

[38] Chiu YM, Chen DY. Infection risk in patients undergoing treatment for inflammatory arthritis: non-biologics versus biologics. Expert Rev Clin Immunol 2020;16(2):207–228. doi:10.1080/1744666X.2019.1705785, PMID:31852268.

[39] Mok TC, Mok CC. Non-TNF biologics and their biosimilars in rheumatoid arthritis. Expert Opin Biol Ther 2024;24(7):599–613. doi:10.1080/14712598.2024.2358165, PMID:38766765.

[40] Meng Q, Wei K, Shan Y. E3 ubiquitin ligase gene BIRC3 modulates TNF-induced cell death pathways and promotes aberrant proliferation in rheumatoid arthritis fibroblast-like synoviocytes. Front Immunol 2024;15:1433898. doi:10.3389/fimmu.2024.1433898, PMID:39301019.

[41] de Seabra Rodrigues Dias IR, Lo HH, Zhang K, Law BYK, Nasim AA, Chung SK, *et al*. Potential therapeutic compounds from traditional Chinese medicine targeting endoplasmic reticulum stress to alleviate rheumatoid arthritis. Pharmacol Res 2021;170:105696. doi:10.1016/j.phrs.2021.105696, PMID:34052360.

[42] Miglioranza Scavuzzi B, Holoshitz J. Endoplasmic Reticulum Stress, Oxidative Stress, and Rheumatic Diseases. Antioxidants (Basel) 2022;11(7):1306. doi:10.3390/antiox11071306, PMID:35883795.

[43] Li Z, Chen M, Wang Z, Fan Q, Lin Z, Tao X, *et al*. Berberine inhibits RA-FLS cell proliferation and adhesion by regulating RAS/MAPK/FOXO/HIF-1 signal pathway in the treatment of rheumatoid arthritis. Bone Joint Res 2023;12(2):91–102. doi:10.1302/2046-3758.122.BJR-2022-0269.R1, PMID:36718649.

[44] Zhang X, Shamsodin M, Wang H, NoormohammadiArani O, Khan AM, Habibi M, *et al*. Dynamic information of the time-dependent tobullian biomolecular structure using a high-accuracy size-dependent theory. J Biomol Struct Dyn 2021;39(9):3128–3143. doi:10.1080/07391102.2020.1760939, PMID:32338161.

[45] Zare-Feizabadi N, Amiri-Tehranizadeh Z, Sharifi-Rad A, Mokaberi P, Nosrati N, Hashemzadeh F, *et al*. Determining the Interaction Behavior of Calf Thymus DNA with Anastrozole in the Presence of Histone H1: Spectroscopies and Cell Viability of MCF-7 Cell Line Investigations. DNA Cell Biol 2021;40(8):1039–1051. doi:10.1089/dna.2021.0052, PMID:34165362.

[46] Marjani N, Dareini M, Asadzade-Lotfabad M, Pejhan M, Mokaberi P, Amiri-Tehranizadeh Z, *et al*. Evaluation of the binding effect and cytotoxicity assay of 2-Ethyl-5-(4-methylphenyl) pyramido pyrazole ophthalazine trione on calf thymus DNA: spectroscopic, calorimetric, and molecular dynamics approaches. Luminescence 2022;37(2):310–322. doi:10.1002/bio.4173, PMID:34862709.

[47] Assaran Darban R, Shareghi B, Asoodeh A, Chamani J. Multi-spectroscopic and molecular modeling studies of interaction between two different angiotensin I converting enzyme inhibitory peptides from gluten hydrolysate and human serum albumin. J Biomol Struct Dyn 2017;35(16):3648–3662. doi:10.1080/07391102.2016.1264892, PMID:27897084.